Inclusive π^0 Production over Large $X_\perp$ and X_F Ranges in 200-, 300-, and 400-GeV/c Proton-Beryllium Interactions

R. M. Baltrusaitis, M. Binkley, B. Cox, T. Kondo, C. T. Murphy, and W. Yang
Fermi National Accelerator Laboratory, Batavia, Illinois 60510

and

L. Ettlinger,[a] M. S. Goodman,[b] J. A. J. Matthews, and J. Nagy[c]
Department of Physics, The Johns Hopkins University, Baltimore, Maryland 21218

(Received 25 June 1979)

Measurements of recognized π^0 production in p-Be collisions for $0.1 < X_\perp < 0.5$ and $-0.8 < X_F < 0.0$ at 200, 300, and 400 GeV/c are presented. These invariant cross sections are fitted by $E\,d\sigma/dp^3 = A(1-X_R)^M P_\perp^{-N}$ over this range of $X_\perp$ and X_F with $M = 4.88 \pm 0.14$ and $N = 8.90 \pm 0.10$ independent of energy. No significant evidence for breaking of this scaling is observed over this large kinematic region at these energies.

The measurement of high-$P_\perp$ and large-X_F inclusive production of π^0's in pN collisions has been the object of a number of experiments at Fermilab[1-8] and the CERN intersecting storage rings (ISR).[9-17] These experiments have attempted to determine whether the invariant cross section can be described over the entire kinematic range and at all energies by a factorized scaling form[18-21] in $P_\perp$ and the radial scaling variable $X_R = (X_F^2 + X_\perp^2)^{1/2}$. We report the results of a measurement of $E\,d\sigma/d^3p$ over a large range of $P_\perp$ and X_R at 200, 300, and 400 GeV/c in the halo-free proton beam[22] of the west branch of the proton area at Fermilab. We have compared these cross sections with the explicit form

$$E\,d\sigma/d^3p = AP_\perp^{-N}(1-X_R)^M. \quad (1)$$

The experimental apparatus, shown in Fig. 1, consisted of a two-arm photon spectrometer. Each arm contained collimators, a 10-kG·m sweeping magnet, a six-plane multiwire proportional chamber system, and a 25-element lead glass Cherenkov counter array along with Lucite (L1, L2, L3) and scintillation (S1, S2) counters. The lead glass arrays were 260 and 240 in. from the thin transmission targets, having 2.0 and 2.6

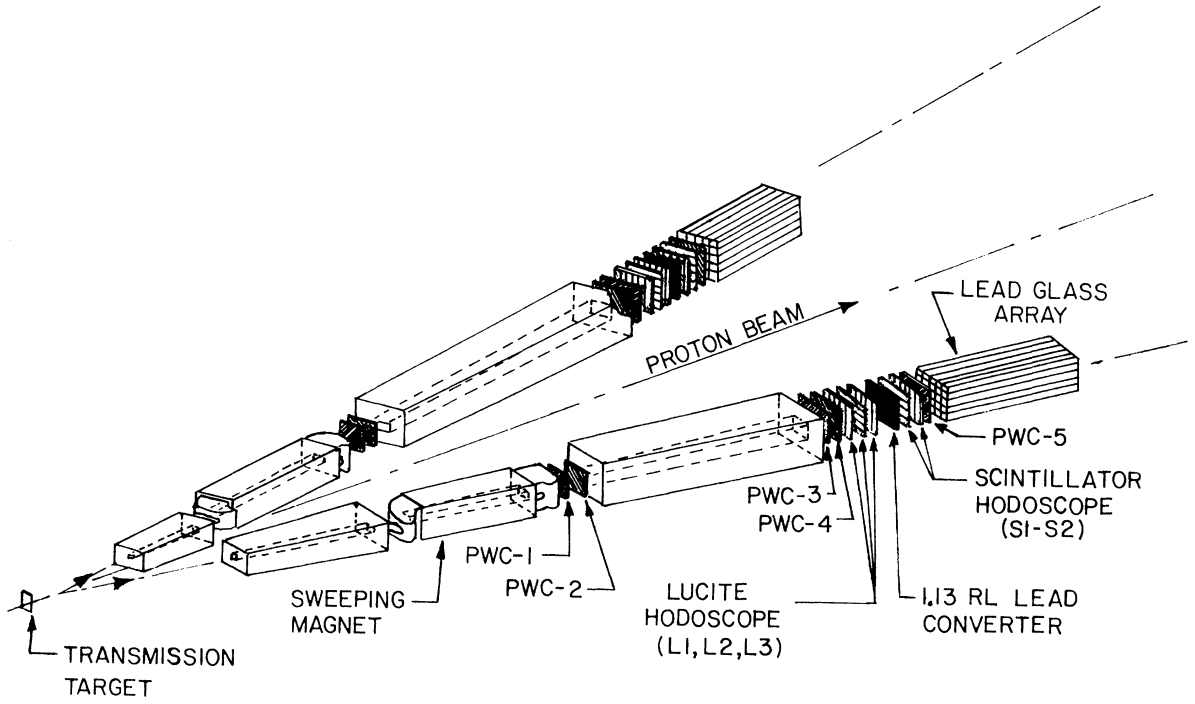

FIG. 1. Schematic view of the double-arm spectrometer.

msr of acceptance, respectively. The two photons from π^0's were both detected in one or the other of the two arms of the spectrometer which were triggered independently. Data were taken at 200, 300, and 400 GeV with the arm angles varied from 5.8° to 18.5° in the laboratory system (90°–150° c.m. system). Thin foil beryllium targets (8 and 34 mil) were used and the cross sections per nucleon are quoted on the assumption of a linear A dependence.[23] The trigger for the π^0 events consisted of the requirement that no charged particle be seen in the Lucite hodoscope (L1 and L2 off) and that a minimum energy be observed in the lead glass array. The cross sections independently determined from each arm agree within assigned errors.

The position of each of the photons from the π^0 decay was determined[24] by fitting the observed fractional energy deposit in each $2\frac{1}{2}$ by $2\frac{1}{2}$ by 24 in.^{3} (24 radiation lengths) element of the lead glass array with the predictions obtained from shower calculations.[25] These calculations were checked by measurements of the actual transverse shower development produced by 4- to 32-GeV/c electrons from an electron beam[26] which was constructed from elements of the "P-West" proton transport in order to allow calibration *in situ* of the detector. The achievable position resolution for the array was approximately $\sigma \sim 0.25$ in.

The linearity of the lead glass array was measured to be better than 0.5% up to 30 GeV by use of the calibration beam. Each of the elements of the array was calibrated before and after each run with this same beam. The gains of each phototube were tracked between these calibrations with a set of hydrogen thyratron light sources monitored against a standard ^{241}Am source. By these techniques the mass of the π^0 peak could be kept stable to ± 1%. Shifts of gains due to beam loading were observed to average less than 1% over the arrays. The fundamental resolution of the lead glass counters was measured[27] to be $\sigma = (7.5\ \mathrm{GeV}^{1/2})/E^{1/2}$ %.

The incident proton flux, which varied from 10^{10} to 10^{12} protons per 1-sec spill during the course of the running, was measured by two secondary-emission monitors. The systematic error in the absolute measurement of flux is estimated to be less than 5%. The dead time was constantly monitored for each data set and was of order 20% for the inclusive π^0 measurement. The probability that a π^0 event was vetoed by the presence of charged particles was monitored by measuring the fluxes of charged particles in the nontriggered arm. The correction to the cross section is typically 10% for these data. Finally, the loss of data due to conversions of one or both of the two

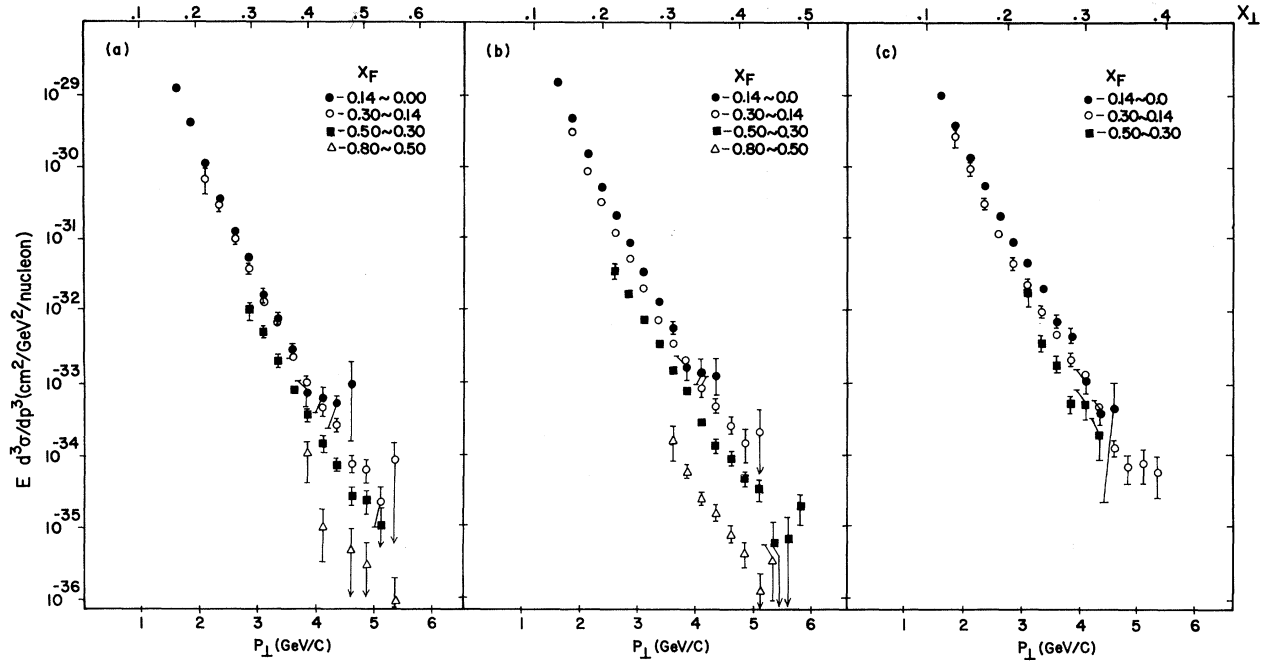

FIG. 2. (a) Invariant cross section $E\,d\sigma/dp^3$ per nucleon vs $P_\perp$ in bands of X_F for p-Be collisions at 200 GeV. Linear A dependence is assumed. (b) 300-GeV cross section. (c) 400-GeV cross section.

TABLE I. Summary of the two-dimensional fits of $E\,d\sigma/dp^3$ ($\mathrm{cm}^2/\mathrm{GeV}^2$ · nucleon) by the form $A(1-X_R)^M P_\perp^{-N}$ at 200, 300, and 400 GeV/c.

Energy (GeV)	$A/10^{-27}$	M	N	χ^2 per degree of freedom
200	3.12 ± 0.22	4.81 ± 0.16	8.90 ± 0.12	1.30
300	3.80 ± 0.21	4.91 ± 0.11	8.93 ± 0.08	1.39
400	2.91 ± 0.22	4.94 ± 0.45	8.79 ± 0.17	1.63

π^0 photons has been corrected by measuring the conversion probability in the front two layers of the Lucite hodoscope for photons from π^0's for data samples which require only a total-energy trigger. This probability was measured to be (16 ± 2)% for a single photon independent of photon energy.

The two-photon background shapes for each two-photon mass spectrum were calculated assuming that the two photons were from uncorrelated π^0's, with the observed inclusive $P_\perp$ and X_F distributions. The fitted backgrounds under the π^0, which depended mainly on threshold energy and were independent of arm angle, ranged from 20% at low thresholds to 5% for data sets with higher thresholds.

In Figs. 2(a), 2(b), and 2(c) the invariant cross section $E\,d\sigma/d^3p$ is displayed as a function of $P_\perp$ for bands of X_F for the three beam energies used in this experiment. The relatively gentle variation of $E\,d\sigma/d^3p$ with X_F can be seen at all three beam energies. A two-dimensional fit of the cross section as function of X_R and $P_\perp$ has been made independently for each energy with the form Eq. (1). The results are given in Table I. If data are distributed in X_R and $P_\perp$ according to Eq. (1) then the product $P_\perp{}^N E\,d\sigma/d^3p$ should be a function only of X_R and therefore be independent of center-of-mass angle of the π^0 ($\theta_{\mathrm{c.m.}}$) at fixed X_R. In Fig. 3(a) the product $P_\perp{}^{9.0} E\,d\sigma/d^3p$ is displayed as a function of $\theta_{\mathrm{c.m.}}$ for different X_R bands for the 200-GeV/c data. The distributions are flat, demonstrating the $\theta_{\mathrm{c.m.}}$ independence of the data.

Furthermore, if Eq. (1) describes the cross section for π^0 production, then $(1-X_R)^{-M} E\,d\sigma/d^3p$ vs $P_\perp$ will explicitly display the $P_\perp$ dependence of the data. In Fig. 3(b) this product (with M set equal to 5 as indicated by the two-dimensional fits) is plotted versus $P_\perp$ for the three beam energies used in the experiment. The $P_\perp{}^{-9}$ behavior and the equality of the cross sections can

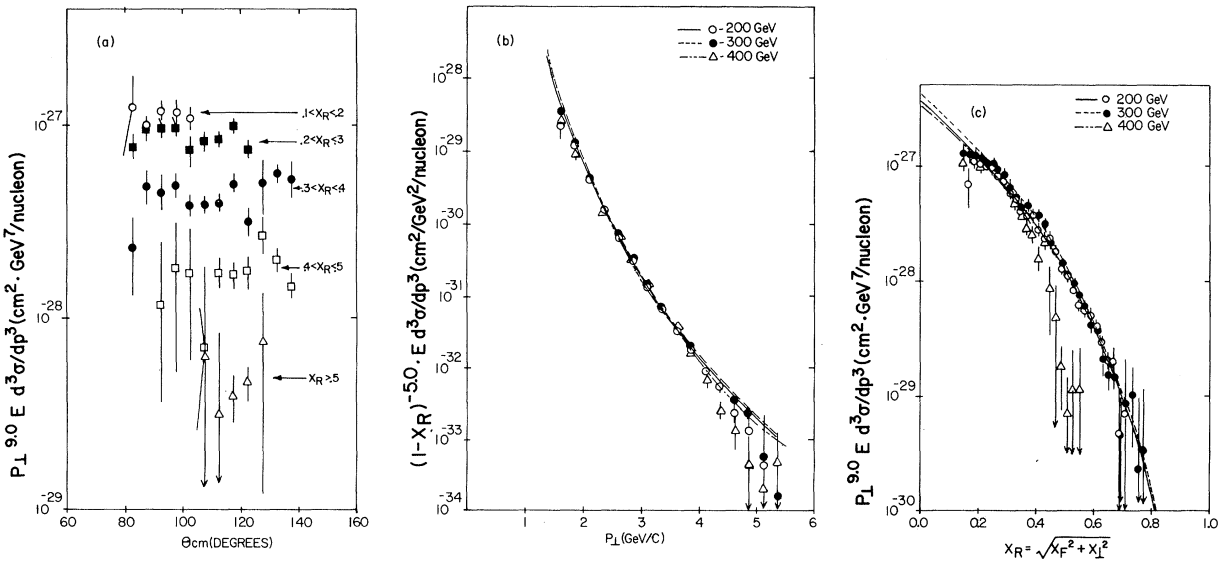

FIG. 3. (a) $P_\perp{}^9 E\,d\sigma/dp^3$ vs $\theta_{\mathrm{c.m.}}$ at 200 GeV/c for various regions of X_{radial}. (b) $(1-X_R)^{-5} E\,d\sigma/dp^3$ vs $P_\perp$ for 200, 300, and 400 GeV/c. (c) $P_\perp{}^9 E\,d\sigma/dp^3$ vs X_R for 200-, 300-, and 400-GeV/c data. Fits to each data set are shown.

clearly be seen at all energies.

Finally, the complementary plot to Fig. 3(b) is the plot of $P_\perp{}^9 E\, d\sigma/d^3p$ vs X_R. The variation of this product with X_R is shown for the three beam energies in Fig. 3(c). As is shown in Fig. 3(c) and recorded in Table I, $(1-X_R)^{4.9}$ is the preferred fit for all energies but the data may be somewhat steeper at 400 GeV/c for the few low-statistics, high-X_R points.

In conclusion, over a large range of X_F and $P_\perp$ we have observed scaling and factorization of the π^0 inclusive cross section as a universal function of X_R and $P_\perp$ at 200, 300, and 400 GeV/c. We observe a much flatter X_R (equivalent to $X_\perp$ at 90° center-of-mass system) dependence than that reported by experiments performed at 90°.[1,5,9-17] Our result is in agreement with the recent experiment of Donaldson *et al.*,[4] performed at 100 and 200 GeV/c over X_F and $P_\perp$ ranges comparable to our experiment. Secondly, we observe no flattening of the $P_\perp$ distribution of the cross section over an $X_\perp$ range comparable to that of the recent ISR experiments[11,17] which report a change in $P_\perp$ exponent from 9 to ~5 as $P_\perp$ increases. We conclude that the phenomenon observed at the ISR is due either to the high $P_\perp$ or the large $s^{1/2}$ rather than to the large $X_\perp$ of their data.

We would like to express our thanks to the Fermilab Proton Department. We wish to acknowledge the many contributions of Leon Madansky and early support of T. Toohig, A. Pevsner, C. Y. Chien, and B. Barnett. This work was supported in part by the U. S. Department of Energy, the Research Corporation of America, and The National Science Foundation.

[a]Present address: Mitre Corporation, Metrek Division, McLean, Va. 22101.

[b]Present address: Harvard University, Physics Department, Cambridge, Mass. 02138.

[c]Present address: Brookhaven National Laboratory, Upton, N. Y. 11973.

[1]J. W. Cronin *et al.*, Phys. Rev. D 11, 3105 (1975).

[2]G. Donaldson *et al.*, Phys. Rev. Lett. 36, 1110 (1976).

[3]G. Donaldson *et al.*, Phys. Rev. Lett. 40, 917 (1978).

[4]G. Donaldson *et al.*, Phys. Lett. 73B, 375 (1978).

[5]D. Antreasyan *et al.*, Phys. Rev. Lett. 38, 105 (1977).

[6]D. C. Carey *et al.*, Phys. Rev. Lett. 33, 327 (1974).

[7]D. C. Carey *et al.*, Phys. Rev. Lett. 33, 330 (1974).

[8]F. E. Taylor *et al.*, Phys. Rev. D 14, 1217 (1976).

[9]F. W. Büsser *et al.*, Phys. Lett. 46B, 471 (1973).

[10]F. W. Büsser *et al.*, Nucl. Phys. B106, 1 (1976).

[11]A. L. S. Angelis *et al.*, Phys. Lett. 79B, 505 (1978).

[12]K. Eggert *et al.*, Nucl. Phys. B98, 49 (1975).

[13]K. Eggert *et al.*, Nucl. Phys. B98, 73 (1975).

[14]A. G. Clark *et al.*, Nucl. Phys. B142, 180 (1978).

[15]A. G. Clark *et al.*, Phys. Lett. 74B, 267 (1978).

[16]C. Kourkoumelis *et al.*, CERN Report No. EP 79-12, 1979 (unpublished).

[17]C. Kourkoumelis *et al.*, CERN Report No. EP 79-29, 1979 (unpublished).

[18]R. P. Feynman, Phys. Rev. Lett. 23, 2159 (1969).

[19]K. Kinoshita and H. Noda, Prog. Theor. Phys. 46, 1639 (1971).

[20]K. Kinoshita and H. Noda, Prog. Theor. Phys. 49, 896 (1973).

[21]K. Kinoshita and H. Noda, Prog. Theor. Phys. 50, 915 (1973).

[22]B. Cox and C. T. Murphy, Nucl. Instrum. Methods 136, 35 (1976).

[23]R. M. Baltrusaitis *et al.*, Fermilab Report No. Pub. 79/39-Exp. (to be published).

[24]R. M. Baltrusaitis *et al.*, "Position determination of high energy photons in lead glass," to be published.

[25]U. Völkel, DESY Report No. 67/16, 1967 (unpublished).

[26]B. Cox *et al.*, Fermilab Report No. TM-765, 6038.00 (unpublished).

[27]M. S. Goodman *et al.*, unpublished.